

Theoretical Study of The Ratio A/A_s Effect on Saturable Absorber Performance of Passive Q-switched Tm^{+3} Doped Fiber Laser System

Tahani M. Hussein ^{1a}, Abdul - Kareem Mahdi Salih ^{1b*} and M. Benhaliliba ^{2c}

¹ Department of Physics, College of Science, University of Thi-Qar, Thi-Qar, Iraq.

² Film Device Fabrication–Characterization and Application FDFCA Research Group USTOMB, 31130, Oran, Algeria.

^aEmail: tahaniilaser@gmail.com & tahaniimohmed739@gmail.com

^cEmail: mostefa.benhaliliba@univ-usto.dz

^{b*}Corresponding author: karimmahdisalih@yahoo.co.uk & abdulkareem@sci.utq.edu.iq

Received:2024-5-27, Revised:2024-08-02, Accepted: 2024-08-08, Published: 2024-12-30

Abstract— The effect of the ratio of active media effective area to the saturable absorber effective area (A/A_s) on saturable absorber performance has been studied numerically for passive Q-switching fiber laser system doped with Tm^{+3} as an active medium and Cr^{+4} :YAG crystal as a saturable absorber. Software program using Rang- Kutta-Fehlberge numerical method prepared in the study to carry out the simulation. The simulation shows that the increasing A/A_s value results in the generation of passive Q-witched pulses in shorter times, allowing optical bleaching of the saturable absorber material and convergence between ground absorption activity and excited levels occurs earlier in time.

Keywords—High power pulses, Passive Q-switching, Fiber Laser, Tm^{+3} , Cr^{+4} :YAG

I. INTRODUCTION

For many applications, Q-switched fiber lasers are the most desired laser sources because of their ability to generate high energy pulses including sensors, micromachining, and medical systems, and material processing [1,2]. Passive Q-switching technique based on saturable absorbers (SAs) has been a popular technique used with fiber as an active medium doped with rare earth element ions to generate short pulses characterized by high power [3]. Thulium (Tm^{+3}) is an effective element laser medium; it is classified in the lanthanide group of the rare earth metal. It is often used to doped optical fiber, due the higher levels ions via energy transfer processes which are leads to the creation of color centers which significantly increase the absorption [4]. So, it has good efficiency compared to another optical fiber laser [5,6]. Figure(1) shows the energy level diagram of Tm^{+3} [7].

Cr^{4+} :YAG crystal characterized by high absorption in the first time and became bleaching or low absorption, and the laser photons passé through it. And have been widely used as a saturable absorbers (SA) for passively Q-switched laser generation [8,9], at the laser wavelength, the crystal exhibit a wide absorption cross section and a low saturable. Also has been effectively used as passive Q-

switches for different active media. Cr^{+4} :YAG energy levels diagram is shown in Figure (2) [10].

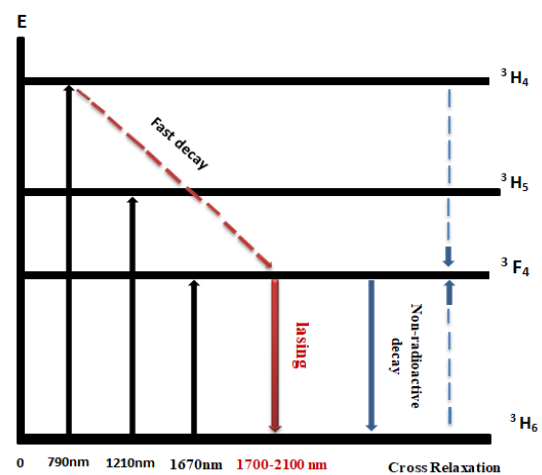


Fig. (1): Energy level diagram of (Tm^{+3}) [7]

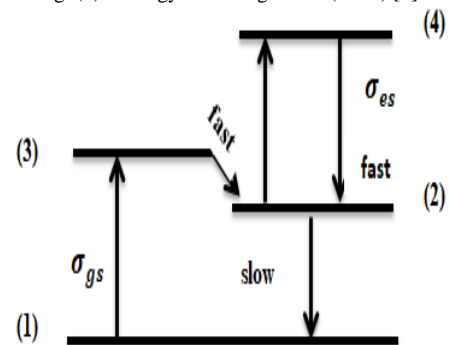


Fig. (2): Energy level diagram of Cr^{+4} :YAG [10]

In this study, we focusing about the ratio effect of effective aria of AM (A) to the the effective aria of SA(A_s) on saturable absorber performance of passive Q-switched Tm^{+3} doped Fiber laser system. Where A and A_s , can be

chooses by controlling the dimensions of the resonator, the effective medium, and the diameter of the mirrors.

II. THEORY

The model of coupled rate equations [11] has been used to study the effect of the ratio of effective area in active medium AM to the effective area in SA on the absorption behavior of SA as the following rate equations model.

$$\frac{d\phi(t)}{dt} = \frac{\phi(t)}{\tau_r} [2\sigma_{am} l_{am} N(t) - 2\sigma_{gs} l_{sa} n_{gs}(t) - 2\sigma_{es} l_{sa} n_{es}(t) - (\ln(\frac{1}{R}) + L_{loss})] \quad (1)$$

$$\frac{dN(t)}{dt} = R_p - \gamma c \sigma_{am} \phi(t) N(t) - \frac{N(t)}{\tau_{am}} \quad (2)$$

$$\frac{dn_{gs}(t)}{dt} = \frac{n_{gs}(t)}{\tau_{sa}} - (2\sigma_{gs} l_{sa} \phi(t) n_{gs}(t) / \tau_r) (A / A_s) \quad (3)$$

$$\frac{dn_{es}(t)}{dt} = -\frac{n_{es}(t)}{\tau_{sa}} + (2\sigma_{es} l_{sa} \phi(t) n_{es}(t) / \tau_r) (A / A_s) \quad (4)$$

Where: ϕ (cm^{-3}) is the photons number density, $\tau_r = 2l_{am} / c$ (s) is the transit time for one round-trip, l_r (cm) is the length of the optical cavity, σ_{am} (cm^2) is the active medium emission cross section, c (ms^{-1}) is the light speed, σ_{gs} (cm^2) is the absorption cross section of SA ground-state, l_{am} (cm) is the length of AM, l_{sa} (cm) is the length of SA, n_{gs} (cm^{-3}) is the SA ground state population, N (cm^{-3}) is the active medium population inversion density, n_{es} (cm^{-3}) is the SA excited state population, $R = (R_1 R_2)^{1/2}$ is the geometric mean of the cavity, $R_1 R_2$ is the reflectivity of mirrors, L_{loss} is the dissipative optical losses for round-trip. N (cm^{-3}) is the population inversion density, σ_{es} (cm^2) is the absorption cross section of SA excited-state, γ is the factor of population reduction equal 1 for 4 levels system, and 2 for 3 system level of active medium, R_p is the rate of optical pumping, τ_{sa} (s) is the lifetime of the excited level of SA, τ_{am} (s) is the fluorescence lifetime of the upper laser level. A is the effective area of AM, A_s is the effective area of SA.

SA's lifetime with Q-switched laser pulses typically has a very short build-up time [12] compared to the fluorescence life of the upper laser level, so it is possible to ignore the spontaneous decay in AM and SA. Additionally, the pumping rate during pulse generation is much longer when compared to the build-up time of Q-switched laser pulses [13]; then Eq.(2), Eq.(3), and Eq.(4) can be reformulation as the below respectively:

$$\frac{dN(t)}{dt} = -\gamma c \sigma_{am} \phi(t) N(t) \quad (5)$$

$$\frac{dn_{gs}(t)}{dt} = (-2\sigma_{gs} l_{sa} \phi(t) n_{gs}(t) / \tau_r) (A / A_s) \quad (6)$$

$$\frac{dn_{es}(t)}{dt} = (2\sigma_{es} l_{sa} \phi(t) n_{es}(t) / \tau_r) (A / A_s)$$

(7)

At the beginning of the optical cavity, the density of photons is at its lowest and the majority of SA molecules are in their ground state (n_{gs}). As a result, the total number of SA molecules can be expressed as ($n_{so} = n_{gs} + n_{es}$), where ($n_{gs} \approx n_{so}$, $n_{es} \approx 0$). At first, the SA absorption activity is also quite high; this can be considered $d\phi / dt \approx 0$ from Eq. (1), but it cannot be considered $\phi(t) = 0$. Then;

$$2\sigma_{am} l_{am} N_o - 2\sigma_{gs} l_{sa} n_{so} - (\ln(\frac{1}{R}) + L_{loss}) = 0 \quad (8)$$

From Eq.(1), at the initial time of the pulse can be regarded $N(t) \approx Loss(t)$, and $\frac{d\phi}{dt} \approx 0$, then can be write:

$$Loss(t) = [2\sigma_{gs} l_{sa} n_{gs}(t) + 2\sigma_{es} l_{sa} n_{es}(t) + (\ln(\frac{1}{R}) + Loss)] / (2\sigma_{am} l_{am}) \quad (9)$$

The ground state of SA is represented by the first term of Eq. (9) as photon absorption, while the excited state of SA is represented by the second term as the following formulas:

$$Absg(t) = 2\sigma_{gs} l_{sa} n_{gs}(t) / (2\sigma_{am} l_{am}) \quad (10)$$

$$Abse(t) = 2\sigma_{es} l_{sa} n_{es}(t) / (2\sigma_{am} l_{am}) \quad (11)$$

The summation of Eq.(10) and Eq.(11) get the total photons absorption in SA :

$$Tabs = \frac{(2\sigma_{gs} l_{sa} n_{gs}(t) + 2\sigma_{es} l_{sa} n_{es}(t))}{2\sigma_{am} l_{am}} \quad (12)$$

When may be taken as a maximum of ϕ and that mean $n_{es} \approx n_{so}$ can be disregarded n_{gs} from Equation (1), the threshold population inversion density can be estimated using the following expression:

$$N_{th} = \frac{2\sigma_{es} n_{so} l_{sa} + \ln(\frac{1}{R}) + L_{loss}}{2\sigma_{am} l_{am}} \quad (13)$$

III. RESULTS AND DISCUSSION

A software program was created specifically for this work to use the Rung-Kutta-Fehlberge method to numerically solve the rate equations (1,5-7). The table (1) displays the input data that was used:

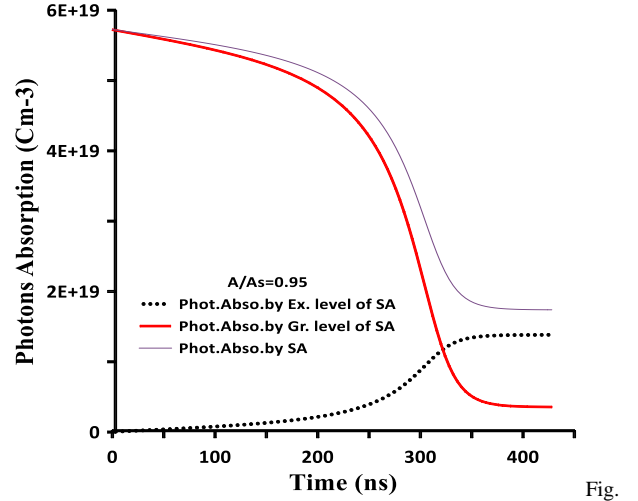
Table (1) : The input data

Parameter	Refer.	Parameter	Refer.	Parameter	Refer.
$l_{am} = 25 \text{ cm}$	14	$R 1 = 90 \%$	15	$t_{sa} = 4.0 \times 10^{-6} \text{ s}$	16
$\sigma_{am} = 0.46 \times 10^{-20} \text{ cm}^2$		$R 2 = 95 \%$		$\sigma_{es} = 2.25 \times 10^{-19} \text{ cm}^2$	17
$\lambda = 1875 \text{ nm}$		$l_r = 300 \text{ cm}$		$N_i = 3.014 \times 10^{-19} \text{ cm}^{-3}$	
$\tau_{am} = 2.38 \times 10^{-3} \text{ s}$				$\sigma_{gs} = 8.75 \times 10^{-19} \text{ cm}^2$	

Figure (3) shows the case that the absorption activity converges time of both levels (AACT) for each of the two levels occurs at approximately 376 ns, where the intensity of photons absorption (IPA) at the absorption activity converges time is approximately in the ground level 1.12×10^{19} and in the excited level 1.18×10^{19} roughly, and that the state of optical bleaching (OP) occurs at around 464 ns. Figure (4), depicts at a value of $A/A_s = 0.95$, that the activities of the SA referred to above occur at previous time comparing with the case of at $A/A_s = 0.9$ as seen in Figure (3). The case of AACT of both levels takes place at a about 322 ns at $A/A_s = 0.95$, where the IPA at absorption activity converges time is approximately 1.154×10^{19} in the ground level and in the excited level approximately 1.151×10^{19} , and the OP occurs at approximately 388 ns.

Figure (5) shows at the value of $A/A_s = 1$, that the AACT of both levels takes place about 288 ns, where the IPA at the absorption activity converges time approximately 1.132×10^{19} in the ground level and approximately 1.133×10^{19} in the excited level. The state of OP occurs at time approximately 360 ns.

It is clear from the results of figures (3-5) that the optical bleaching of the absorbent material and the state of convergence of the density of the absorbed photons in each of the two SA levels occur at advanced times as the value of A/A_s increases. In table (2), we briefly present these results.



(4): The time variation of photons Absorption density at $A/A_s=0.95$

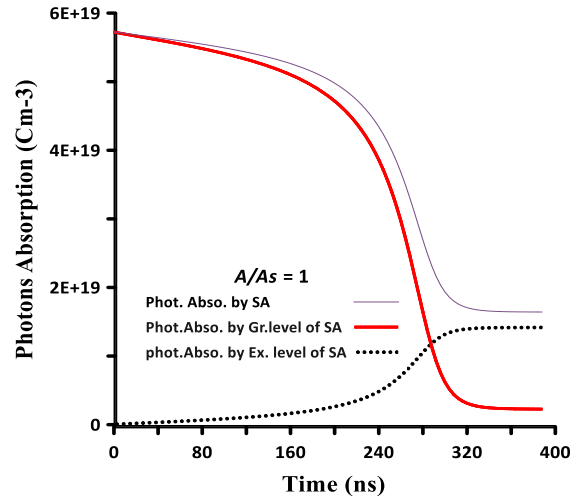


Fig (5): The time variation of photon absorption density at $A/A_s=1$

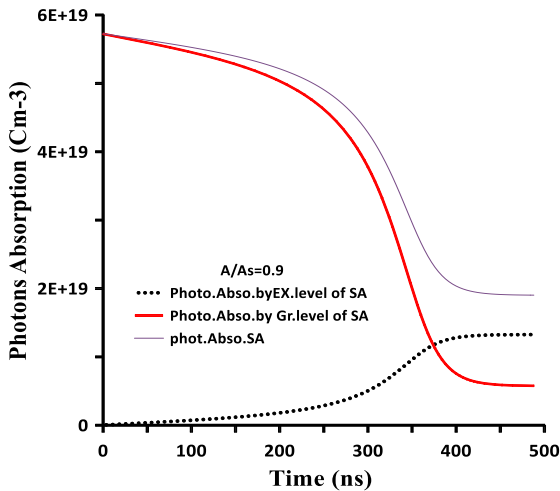


Fig. (3): The time variation of photons absorption density at $A/A_s=0.9$

Then the performance of SA according to A/A_s value leads to the emission of the passively Q-switched pulse at an advanced time and characterized by less duration and more energy as the value of A/A_s increases, this results shown in figure (6a), where is clear from the figure, the pulse emission times approximately are 307ns, 334ns, and 372 ns respectively, also it is clear from the figure (6) the duration time is decrease with the increasing of A/A_s .

That is lead to high power pulse. For further clarification and verification, figures (7-9) demonstrate the temporal behavior of the performance of each of the ground level, excited and the total performance of the absorbent material, respectively, with regard to the absorption of laser photons. Where the occurrence of optical bleaching appears in advanced times with the increase in the value of A/A_s .

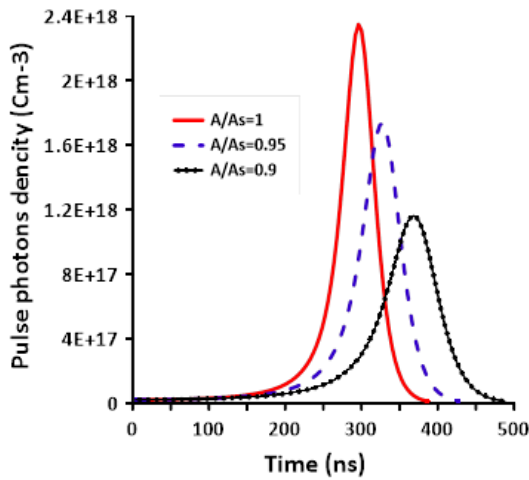


Fig. (6): Pulse photons density as a function of A/A

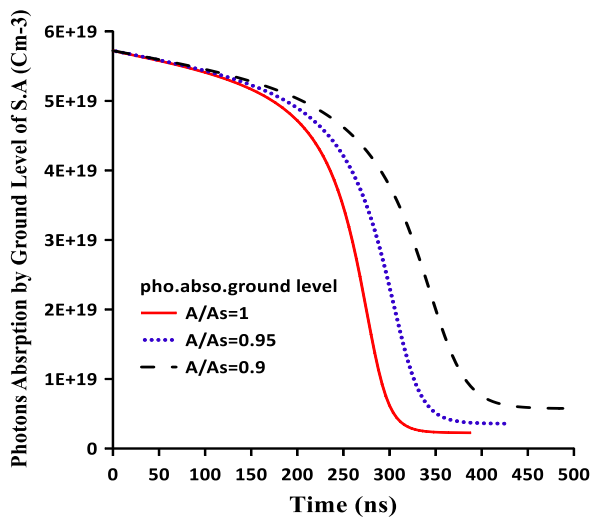


Fig. (7): Photons absorption by the ground level as a function of A/A_s

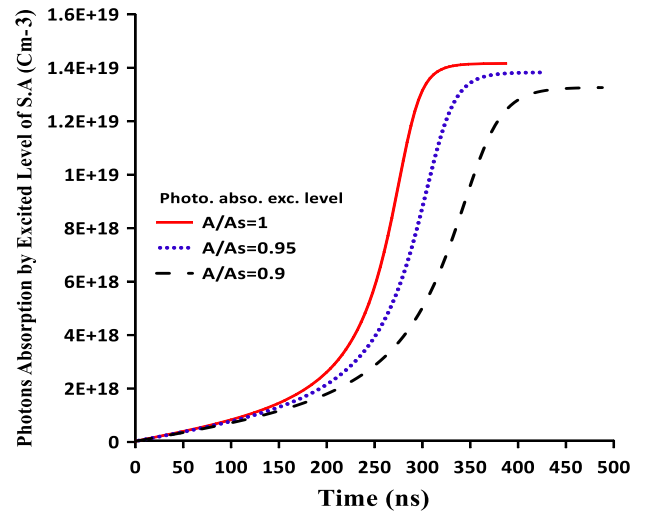


Fig. (8): Photons absorption in excited level as a function of A/A_s

Table (2) : Comparisson of the results between the ground and excited level of SA as a function of A/A_s

A/A_s	Ground level of SA			Excited level of SA		
	0.9	0.95	1	0.9	0.95	1
AACT	376	322	288	376	322	288
IPA(10^{+19} cm ³) at AACT	1,12	1.154	1.132	1.18	1.151	1.33
OP occur at time (ns)	464	388	360	464	388	360

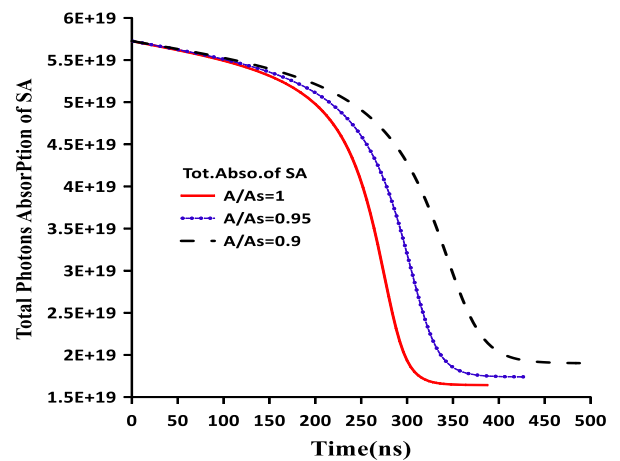


Fig. (9): Total photons absorption in SA as a function of A/A_s

The results of the physical behavior in the figures are explained due to the decreasing and increasing population of the ground level and the excited level in equality, respectively, with the time of increasing the value of (A/A_s) as shown in figure (10) and figure (11).

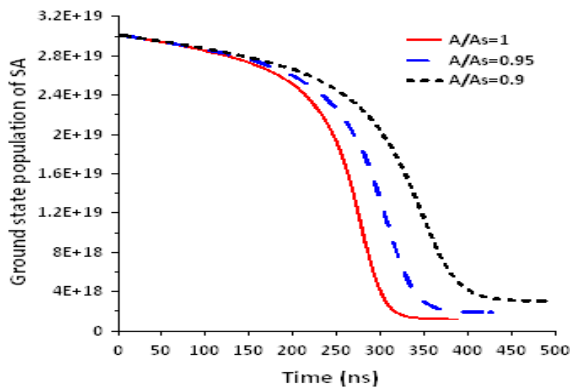


Fig. (10): Ground state population of SA as a function of time.

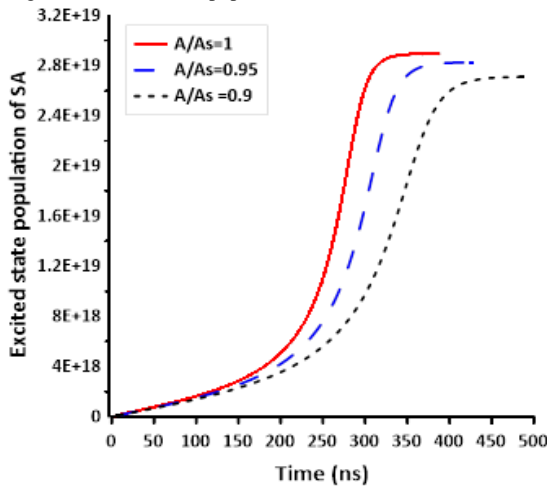


Fig. (11): Excited state population of SA as a function of time.

IV. CONCLUSIONS

The increasing of the A/A_s value leads to the generation of passive Q-switching pulse in an earlier time with less duration and more energy and more power of pulses, so the optical bleaching of the saturable absorber material, and the convergence between the absorption activity of the ground and excited levels occur in an advanced time. Also the increasing of the A/A_s value leads to high power pulses due to decrease in pulse duration. Then this study recommends increasing the factor A/A_s because it is more useful practical application

CONFLICT OF INTEREST

Authors declare that they have no conflict of interest

REFERENCES

[1] H. Ahmad, A. Kamely, N. Yusoff, L. Bayang, and M. Z. Samion, "Generation of Q-switched pulses in thulium-doped and thulium/holmium-co-doped fiber lasers using MAX phase (Ti_3AlC_2)," *Scientific reports*, vol. 10, p. 9233, 2020.

[2] Y. Xu, H. Hu, H. Wu, C. Xu, H. Zhang, L. Jin, *et al.*, "Enhancing Q-switched fiber laser performance based on reverse saturable and saturable absorption properties of $CuCrO_2$ nanoparticle-polyimide films,"

ACS Applied Materials & Interfaces, vol. 13, pp. 21748-21755, 2021.

- [3] P. Hu, J. Mao, H. Nie, R. Wang, B. Zhang, T. Li, *et al.*, "Highly stable passively Q-switched erbium-doped all-fiber laser based on niobium diselenide saturable absorber," *Molecules*, vol. 26, p. 4303, 2021.
- [4] M. Schembri, J. Sahu, O. Aboumarzouk, A. Pietropaolo, and B. K. Somani, "Thulium fiber laser: the new kid on the block," *Turkish Journal of Urology*, vol. 46, p. S1, 2020.
- [5] J. M. Adams, "Thulium Mode – Locked Fiber Laser," M.Sc., University of Dayton, Ohio, 2019.
- [6] J. A. Khusid, R. Khargi, B. Seiden, A. S. Sadiq, W. M. Atallah, and M. Gupta, "Thulium fiber laser utilization in urological surgery: A narrative review," *Investigative and Clinical Urology*, vol. 62, p. 136, 2021.
- [7] T. M. Hussein and A.-K. M. Salih, "Simulation of Effective Beam Area Ratio Effect on Characteristics of Passive Q-Switched Fiber Doped Laser," *Journal of Optoelectronics Laser*, vol. 41, pp. 452-461, 2022.
- [8] R. Currey, A. Khademian, and D. Shiner, "Development of a Thulium Fiber Laser for an Atomic Spectroscopy Experiment," *Fibers*, vol. 8, p. 12, 2020.
- [9] S. Hussien and A. Salih, "Absorption Activity Investigation of Saturable Absorber for Dual Wavelengths in Laser Passive Q-Switching System," *Indian Journal of Science and Technology*, vol. 17, pp. 577-582, 2024.
- [10] D. S. Hussein, "Simulation of pulse characteristics of passive Q-switched ytterbium doped fiber laser," M.Sc., University of Thi-Qar, Iraq, 2020.
- [11] V. Pérez-Alonso, R. Weigand, M. Sánchez-Balmaseda, and J. G. Pérez, "Powerful algebraic model to design Q-switched lasers using saturable absorbers," *Optics & Laser Technology*, vol. 164, p. 109506, 2023.
- [12] A. S. Majli and M. S. Abdul-Kareem, "Simulation of active medium emission cross section influence on passive q-switching laser pulse characteristics," *NeuroQuantology*, vol. 18, p. 62, 2020.
- [13] F. B. Slimen, S. Chen, J. Lousteau, Y. Jung, N. White, S. Alam, *et al.*, "Highly efficient Tm³⁺ doped germanate large mode area single mode fiber laser," *Optical Materials Express*, vol. 9, pp. 4115-4125, 2019.
- [14] D. Savastru, S. Miclos, and I. Lancranjan, "Theoretical analysis of a passively q-switched erbium doped fiber laser," *Revista de Tehnologii Neconventionale*, vol. 16, p. 47, 2012.
- [15] M. A. Belov, L. I. Burov, and L. G. Krylova, "Influence of the Cr⁴⁺: YAG saturable absorber parameters on output characteristics of the Nd³⁺: LSB laser in Q-switched regime," *Nonlinear Phenom. Complex Syst*, vol. 18, pp. 140-148, 2015.
- [16] D. Savastru, R. Savastru, S. Miclos, and I. Lancranjan, "Numerical Analysis of Passively Q-switched Er and Yb Doped Fiber Laser," in *PIERS Proceedings*, 2013.